

Axisymmetric spherical-cavity resonator. I. Normal modes

Babak Makkinejad and George W. Ford

Physics Department, University of Michigan, Ann Arbor, Michigan 48109

(Received 20 May 1991)

The problem of the normal modes of electromagnetic oscillations in a spherical-cavity resonator with axisymmetric interior and ideally conducting walls is solved. The method involves the construction of a complete set of solutions of the axisymmetric wave equation in spherical coordinates, a coordinate system in which the equation is not separable. Fitting the boundary conditions at the surface of the sphere results in an equation for the normal modes in the form of the roots of an infinite-dimensional determinant. The determinant is evaluated by the method of successive truncations. Numerical results are presented for the normal modes as a function of the dielectric asymmetry. The field lines for some of the lowest modes and selected choices of parameters are drawn.

I. INTRODUCTION

We consider the problem of normal modes of the electromagnetic oscillations in a spherical resonating cavity filled with an axisymmetric medium, e.g., ruby. This is a specialization of the problem of the scattering by a gyrotropic sphere, discussed by Ford and Werner.¹ The differences lie in the assumed form of the dielectric relation between the displacement vector \mathbf{D} and the electric vector \mathbf{E} , the boundary conditions at the surface of the sphere, and absorption properties of the dielectric. The problem of free oscillations in the interior of a sphere was solved by Macdonald² in 1902: He solved the problem of electromagnetic oscillations for the case of an ideal conducting sphere with a isotropic dielectric interior. He also noted the existence of what we nowadays call TE and TM modes. We shall, therefore, refer to this problem as Macdonald's problem from now on.

The problem that we are solving is then a generalization of Macdonald's problem to the case of an axially symmetric transparent cavity resonator. The basic difficulty of this problem is that there is no coordinate system in which the Maxwell equations are separable and which has both axial and spherical symmetry. In the Ford-Werner paper, it is shown how to surmount this difficulty, and we apply the same techniques here.

The interest in this problem is chiefly due to the experiments of Strayer, Dick, and Tward³ on superconductor-coated microwave cavity resonators with sapphire interiors. The aim of these experimental researches has been the development of stable microwave-frequency standards with very high quality factor. We, therefore, undertook the solution of this problem in order to further the understanding of the experimental results. In fact, we shall compare our theory with the experimental results of Strayer, Dick, and Tward in a later paper.

In Sec. II we write the basic equations for an axisymmetric medium and introduce the vector spherical waves. In Sec. III we construct the general solution of the axisymmetric wave equation inside the sphere, fit the boundary conditions, and derive an equation for the

normal-mode frequencies. In Sec. IV we describe our method of numerical solution and discuss the numerical calculation of normal modes. We present the outcome of these calculations, displaying the normal-mode frequencies as a function of dielectric asymmetry. We draw the electric-field lines for some of the lowest modes.

II. GENERAL EQUATIONS AND FORMULAS

In this section we shall present the general equations for an axisymmetric medium and equations in such material. In Sec. II A we give the Maxwell equations and dielectric relation in an axisymmetric medium. Then, in Sec. II B, we discuss the boundary conditions for a superconductor-coated resonating cavity. In Sec. II C, in order to develop the modern notation that we shall be using in the general problem, we give solutions of the vector-wave equation in spherical coordinates. There we introduce vector spherical waves, giving the essential formulas we need.

A. General equations

The basic equations are the macroscopic Maxwell equations, and we shall write them in Gaussian units. For fields varying harmonically in time [$\mathbf{E}(\mathbf{r}, t) = \mathbf{E}(\mathbf{r})e^{-i\omega t}$], they are

$$\text{curl}\mathbf{E} - i\frac{\omega}{c}\mathbf{B} = 0, \quad \text{curl}\mathbf{B} + i\frac{\omega}{c}\mathbf{D} = 0, \quad (2.1)$$

where \mathbf{B} is the magnetic field, \mathbf{E} is the electric field, and \mathbf{D} is the electric displacement field. Here the first equation is Faraday's law of induction, and the second is Ampère's law. These equations are completed when the dielectric relation between \mathbf{E} and \mathbf{D} field is specified, i.e.,

$$\mathbf{D} = \vec{\epsilon} \cdot \mathbf{E}. \quad (2.2)$$

The dielectric tensor appearing in the dielectric relation (2.2) may, in general, be a complex function of frequency ω . Since we are interested in a transparent medium, we take it to be real and independent of ω for the fre-

quencies of interest.

The most general cylindrically symmetric form that the dielectric tensor can have is the gyrotropic case:

$$\vec{\epsilon} = \begin{pmatrix} \epsilon_{xx} & \epsilon_{xy} & 0 \\ -\epsilon_{xy} & \epsilon_{xx} & 0 \\ 0 & 0 & \epsilon_{zz} \end{pmatrix}. \quad (2.3)$$

The axisymmetric case is for $\epsilon_{xy} = 0$. The isotropic case corresponds to $\epsilon_{xy} = 0$ and $\epsilon_{xx} = \epsilon_{zz} = \epsilon$.

Inside the dielectric, \mathbf{D} must satisfy the equation obtained by eliminating \mathbf{B} from (2.1) and invoking (2.2), i.e.,

$$\text{curl curl} \mathbf{E} - \left[\frac{\omega}{c} \right]^2 \mathbf{D} = 0. \quad (2.4)$$

Here

$$\mathbf{E} = \vec{\epsilon}^{-1} \cdot \mathbf{D}, \quad (2.5)$$

where $\vec{\epsilon}^{-1}$ is the inverse of the dielectric tensor (2.3). It will be convenient to adopt the notation of Ref. 1 and to express the inverse dielectric relation in the axisymmetric case as

$$\mathbf{E} = (\vec{\epsilon}^{-1} \cdot \mathbf{D}) = (\mathbf{D} + \tilde{\gamma} \hat{\mathbf{z}} \cdot \mathbf{D} \hat{\mathbf{z}}) / \tilde{\epsilon}, \quad (2.6)$$

where

$$\tilde{\epsilon} = \epsilon_{xx}, \quad \tilde{\gamma} = \frac{\epsilon_{xx} - \epsilon_{zz}}{\epsilon_{zz}}. \quad (2.7)$$

Substituting the expression (2.6) into (2.4), we obtain

$$\nabla \times \nabla \times (\mathbf{D} + \tilde{\gamma} \hat{\mathbf{z}} \cdot \mathbf{D} \hat{\mathbf{z}}) - \tilde{\epsilon} \left[\frac{\omega}{c} \right]^2 \mathbf{D} = 0. \quad (2.8)$$

We shall call Eq. (2.8) the axisymmetric wave equation.

B. Boundary conditions

We here discuss the boundary conditions to be applied when we consider electromagnetic fields within a cavity. We consider the cavity walls to be ideal conductors. The boundary conditions at the surface of the cavity will then follow from the Maxwell equations (2.1) by standard arguments.⁴ At the surface the tangential component of \mathbf{E} must vanish to avoid having infinite surface currents. For the same reason, the normal component of \mathbf{B} must vanish. Thus we have

$$\hat{\mathbf{n}} \times \mathbf{E}|_{\text{surface}} = 0, \quad \hat{\mathbf{n}} \cdot \mathbf{B}|_{\text{surface}} = 0. \quad (2.9)$$

Here $\hat{\mathbf{n}}$ is a unit normal at the surface. For time-varying fields these boundary conditions are not independent, as we shall later see explicitly.

C. Vector spherical waves

We begin by introducing scalar spherical waves. These are the solutions in spherical coordinates of the scalar-wave equation (Helmholtz's equation):

$$\nabla^2 u + q^2 u = 0. \quad (2.10)$$

The spherical-wave solutions regular at the origin are

$$u_{lm}(qr) = j_l(qr) Y_{lm}(\hat{\mathbf{r}}), \quad l = 0, 1, 2, 3, \dots, \\ m = 0, \pm 1, \dots, \pm l. \quad (2.11)$$

Here j_l is the spherical Bessel function⁵ and Y_{lm} is the (scalar) spherical harmonic.⁶

The vector spherical waves are solutions in spherical coordinates of the vector-wave equation⁷

$$\nabla(\nabla \cdot \mathbf{U}) - \nabla \times (\nabla \times \mathbf{U}) + q^2 \mathbf{U} = 0. \quad (2.12)$$

The identity $\nabla \times (\nabla \times) = \nabla \nabla \cdot - \nabla^2$ shows that this is just the Helmholtz equation (2.10) acting on a vector wave. The vector spherical waves regular at the origin can be expressed in terms of simple vector analytical operations on the scalar spherical waves. They are of three kinds:

$$\mathbf{B}_{lm}(q\mathbf{r}) = (1/q) \nabla u_{lm}, \\ \mathbf{C}_{lm}(q\mathbf{r}) = -i[l(l+1)]^{-1/2} \mathbf{r} \times \nabla u_{lm}, \\ \mathbf{A}_{lm}(q\mathbf{r}) = (i/q) \nabla \times \mathbf{C}_{lm}. \quad (2.13)$$

For $l=0$ the vector spherical waves \mathbf{A}_{lm} and \mathbf{C}_{lm} are identically zero. The set of \mathbf{A}_{lm} , \mathbf{B}_{lm} , and \mathbf{C}_{lm} (with $l=0, 1, 2, \dots$, $m=0, \pm 1, \dots, \pm l$, and the continuous parameter q) form a complete set of basis functions for vector functions of spherical coordinates. The members of this set are linearly independent and have been constructed so as to have the following simple vector analytical properties:

$$\nabla \cdot \mathbf{A}_{lm} = 0, \quad \nabla \cdot \mathbf{B}_{lm} = -qu_{lm}, \quad \nabla \cdot \mathbf{C}_{lm} = 0, \\ \nabla \times \mathbf{A}_{lm} = iq \mathbf{C}_{lm}, \quad \nabla \times \mathbf{B}_{lm} = 0, \quad \nabla \times \mathbf{C}_{lm} = -iq \mathbf{A}_{lm}. \quad (2.14)$$

With the help of well-known formulas from vector analysis,⁴ one can readily verify that these vector fields satisfy the vector-wave equation (2.12).

It is useful to express the vector spherical waves explicitly in terms of vector spherical harmonics.⁸

$$\mathbf{A}_{lm} = \left[\frac{l}{2l+1} \right]^{1/2} j_{l+1}(qr) \mathbf{Y}_{l,l+1}^m(\hat{\mathbf{r}}) \\ - \left[\frac{l+1}{2l+1} \right]^{1/2} j_{l-1}(qr) \mathbf{Y}_{l,l-1}^m(\hat{\mathbf{r}}), \\ \mathbf{B}_{lm} = \left[\frac{l+1}{2l+1} \right]^{1/2} j_{l+1}(qr) \mathbf{Y}_{l,l+1}^m(\hat{\mathbf{r}}) \\ + \left[\frac{l}{2l+1} \right]^{1/2} j_{l-1}(qr) \mathbf{Y}_{l,l-1}^m(\hat{\mathbf{r}}), \\ \mathbf{C}_{lm} = j_l(qr) \mathbf{Y}_{l,l}^m(\mathbf{r}). \quad (2.16)$$

In the application of the boundary conditions, we shall also need the formulas⁹

$$\begin{aligned}\hat{\mathbf{r}} \cdot \mathbf{A}_{lm} &= -[l(l+1)]^{1/2} [j_l(qr)/qr] Y_{lm}(\hat{\mathbf{r}}), \\ \hat{\mathbf{r}} \cdot \mathbf{B}_{lm} &= \left[\frac{d_{jl}(qr)}{d(qr)} \right] Y_{lm}, \\ \hat{\mathbf{r}} \cdot \mathbf{C}_{lm} &= 0,\end{aligned}\quad (2.17)$$

and

$$\begin{aligned}\hat{\mathbf{r}} \times \mathbf{A}_{lm} &= -i \left[\frac{j_l(qr)}{qr} + \frac{dj_l(qr)}{d(qr)} \right] \mathbf{Y}_{ll}^m(\hat{\mathbf{r}}) \\ &\equiv -i\alpha_l(qr) \mathbf{Y}_{ll}^m(\hat{\mathbf{r}}), \\ \hat{\mathbf{r}} \times \mathbf{B}_{lm} &= i[l(l+1)]^{1/2} [j_l(qr)/qr] \mathbf{Y}_{ll}^m(\hat{\mathbf{r}}), \\ \hat{\mathbf{r}} \times \mathbf{C}_{lm} &= ij_l(qr) \left[\left[\frac{l}{2l+1} \right]^{1/2} \mathbf{Y}_{l,l+1}^m(qr) \right. \\ &\quad \left. + \left[\frac{l+1}{2l+1} \right]^{1/2} \mathbf{Y}_{l,l-1}^m(\hat{\mathbf{r}}) \right].\end{aligned}\quad (2.18)$$

III. SOLUTION FOR AN AXISYMMETRIC CAVITY

In this section we shall generalize Macdonald's problem to the case of an axisymmetric spherical-cavity resonator. The cavity is filled with an isotropic, axisymmetric dielectric material, e.g., sapphire. We shall assume the walls of cavity to be ideal conductors, while the material is assumed to be transparent with magnetic permeability $\mu=1$. We take the radius of the cavity to be a .

We begin in Sec. III A by constructing the general regular solution in spherical coordinates of Maxwell equations for an axisymmetric medium. This solution will be in the form of an infinite series of vector spherical waves,

which leads to an eigenvalue problem for the coefficients of the vector spherical waves. In Sec. III B we expand the fields inside the sphere in terms of this solution. We then apply the boundary conditions to obtain an infinite set of coupled homogeneous linear algebraic equations for the expansion coefficients. The roots of the determinant of the coefficients of this set of homogeneous equations give the normal-mode frequencies. In Sec. III C we discuss the auxiliary eigenvalue problem which occurs in the general solution.

A. General solution in an axisymmetric medium

We shall seek a solution of the axisymmetric wave equation (2.8) in the interior of the cavity. We begin by expanding the \mathbf{D} field in a series of vector spherical waves. Since the divergence of \mathbf{D} must be zero, it follows that the vector spherical waves \mathbf{B}_{lm} do not appear in the expansion of the \mathbf{D} field. Thus we may write

$$\mathbf{D}(qr) = \sum_{l,m} [a_{lm} \mathbf{A}_{lm}(qr) + c_{lm} \mathbf{C}_{lm}(qr)], \quad (3.1)$$

where q is as yet unknown and a_{lm} and c_{lm} are the expansion coefficients which are yet to be determined. Here the summation goes from $l=l_{\min}$ to $l=\infty$, where l_{\min} is the larger of m and 1. In order to proceed further, we need the formulas¹⁰

$$\hat{\mathbf{z}} \cdot \mathbf{A}_{lm} \hat{\mathbf{z}} = \sum_{l'} (R_{ll'}^m \mathbf{A}_{l'm} + S_{ll'}^m \mathbf{B}_{l'm} + T_{ll'}^m \mathbf{C}_{l'm}), \quad (3.2)$$

$$\hat{\mathbf{z}} \cdot \mathbf{C}_{lm} \hat{\mathbf{z}} = \sum_{l'} \left[P_{ll'}^m \mathbf{A}_{l'm} + Q_{ll'}^m \mathbf{B}_{l'm} + \frac{m^2}{l(l+1)} \delta_{ll'} \mathbf{C}_{l'm} \right],$$

where

$$\begin{aligned}R_{ll'}^m &= H(l+2, m)H(l+1, m)\delta_{l',l+2} + \left[\frac{l+1}{l+2} H^2(l+1, m) + \frac{l}{l-1} H^2(l, m) \right] \delta_{l',l} + H(l, m)H(l-1, m)\delta_{l',l-2} = R_{ll'}^m, \\ S_{ll'}^m &= - \left[\frac{l+2}{l+3} \right]^{1/2} H(l+1, m)H(l+2, m)\delta_{l',l+2} + [l(l+1)]^{-1/2} \left[\frac{m^2}{l(l+1)} - (l+1)H^2(l+1, m) + lH^2(l, m) \right] \delta_{l',l} \\ &\quad + \left[\frac{l-1}{l+2} \right]^{1/2} H(l, m)H(l-1, m)\delta_{l',l-2}, \\ T_{ll'}^m &= - \frac{m}{(l+2)} H(l+1, m)\delta_{l',l+1} - \frac{m}{(l-1)} H(l, m)\delta_{l',l-1} = P_{ll'}^m, \\ Q_{ll'}^m &= \frac{m}{l} \left[\frac{l+1}{l+2} \right]^{1/2} H(l+1, m)\delta_{l',l+1} - \frac{m}{l+1} \left[\frac{l}{l-1} \right]^{1/2} H(l, m)\delta_{l',l-1},\end{aligned}\quad (3.3)$$

with

$$H(l, m) \equiv \left[\frac{(l^2-1)(l^2-m^2)}{l^2(4l^2-1)} \right]^{1/2}. \quad (3.4)$$

Then inserting the expansion (3.1) into the dielectric relation (2.6) for the \mathbf{D} field and using formulas (3.2) and (3.3), we get

$$\mathbf{D} + \tilde{\gamma} \hat{\mathbf{z}} \cdot \mathbf{D} \hat{\mathbf{z}} = \sum_{l,l'} \left\{ [a_{lm}(\delta_{ll'} + \tilde{\gamma} R_{ll'}^m) + c_{lm} \tilde{\gamma} P_{ll'}^m] \mathbf{A}_{l'm} + \tilde{\gamma} (a_{lm} S_{ll'}^m + c_{lm} Q_{ll'}^m) \mathbf{B}_{l'm} \right. \\ \left. + \left[\tilde{\gamma} a_{lm} T_{ll'}^m + c_{lm} \left[\tilde{\gamma} \frac{-m^2}{l(l+1)} + 1 \right] \delta_{ll'} \right] \mathbf{C}_{l'm} \right\}. \tag{3.5}$$

Next, we put this expression into the axisymmetric wave equation (2.8) and use the expansion (3.1). Then, using the curl formulas (2.15), the axisymmetric wave equation becomes

$$0 = \nabla \times \nabla \times (\mathbf{D} + \tilde{\gamma} \hat{\mathbf{z}} \cdot \mathbf{D} \hat{\mathbf{z}}) - q_0^2 \mathbf{D} \\ = \sum_{l,l'} \left\{ [a_{lm}(\delta_{ll'}(q^2 - q_0^2) + q^2 \tilde{\gamma} R_{ll'}^m) + c_{lm} q^2 \tilde{\gamma} P_{ll'}^m] \mathbf{A}_{l'm} + \left[q^2 \tilde{\gamma} a_{lm} P_{ll'}^m + c_{lm} \left[q^2 \tilde{\gamma} \frac{-m^2}{l(l+1)} \delta_{ll'} + (q^2 - q_0^2) \delta_{ll'} \right] \right] \mathbf{C}_{l'm} \right\}. \tag{3.6}$$

But the vector spherical waves are linearly independent; hence, equating separately the coefficients of \mathbf{A}_{lm} and \mathbf{C}_{lm} to zero, we obtain two infinite sets of equations for the coefficients a_{lm} and c_{lm} ,

$$\sum_{l'} [a_{l',m}(R_{l'l}^m - \mu \delta_{l'l}) + c_{l'm} P_{l'l}^m] = 0, \tag{3.7} \\ \sum_{l'} \left[c_{l'm} \left[\frac{m^2}{l(l+1)} \delta_{l'l} - \mu \delta_{l'l} \right] - a_{l'm} P_{l'l}^m \right] = 0.$$

Here we have defined μ through the relation

$$q^2 = \frac{q_0^2}{1 + \tilde{\gamma} \mu}, \tag{3.8}$$

where $q_0^2 = \epsilon_{xx}(\omega/c)^2$. For every value of μ for which there is a solution of these equations, there will be a corresponding solution of the axisymmetric wave equation, where $0 \leq \mu \leq 1$. We note that (3.8) implies that normal-mode frequencies will be dependent on $\tilde{\gamma}$. Moreover, it suggests the existence of normal-mode frequencies that are independent of $\tilde{\gamma}$ for $\mu = 0$.

Next, we note from the form of matrices given in definitions (3.3) that the matrix $P_{ll'}^m$ connects only values of l and l' with opposite parity, while the matrix $R_{ll'}^m$ connects only values with the same parity. Hence we may classify the solutions of Eqs. (3.7) into two types: *even*, for which $c_{lm} = 0$ for odd l and $a_{lm} = 0$ for even l , and *odd*, for which $a_{lm} = 0$ for odd l and $c_{lm} = 0$ for even l . These two types correspond to odd and even parity for the corresponding \mathbf{D} . Therefore, for the odd solutions we introduce

$$d_{lm}^-(\mu) \equiv \begin{cases} c_{lm}, & l \text{ odd} \\ a_{lm}, & l \text{ even} \end{cases}, \tag{3.9}$$

while for the even solutions we introduce

$$d_{lm}^+(\mu) \equiv \begin{cases} a_{lm}, & l \text{ odd} \\ c_{lm}, & l \text{ even} \end{cases}. \tag{3.10}$$

Then Eqs. (3.7) can be written in the form of an eigenvalue problem:

$$\sum (\mathcal{N}_{ll'}^{m\sigma} - \mu \delta_{ll'}) d_{l'm}^\sigma = 0, \tag{3.11}$$

where $\sigma = \pm$, and

$$\mathcal{N}_{ll'}^{m\sigma} = \begin{cases} -(m/l)H(l+1, m)\delta_{l',l+1} + [m^2/l(l+1)]\delta_{l'l} - [m/(l+1)]H(l, m)\delta_{l',l-1}, & \sigma = (-1)^l, \\ H(l+2, m)H(l+1, m)\delta_{l',l+2} - (m/l+2)H(l+1, m)\delta_{l',l+1}, \\ + \left[\frac{l+1}{l+2} H^2(l+1, m) + \frac{l}{l-1} H^2(l, m) \right] \delta_{l'l} - (m/l-1)H(l, m)\delta_{l',l-1} + H(l, m)H(l-1, m)\delta_{l',l-2}, \\ \sigma = (-1)^{l+1}. \end{cases} \tag{3.12a} \tag{3.12b}$$

The infinite matrix $\mathcal{N}^{m\sigma}$, whose elements are the $\mathcal{N}_{ll'}^{m\sigma}$, is real and symmetric, and so the eigenvalues μ are real. For each m and σ , there is a spectrum of eigenvalues μ . We shall see later that this spectrum is, in fact, continuous, with eigenvalues falling in the region $0 \leq \mu \leq 1$. The solutions of the axisymmetric wave equation (2.8) are labeled by m , σ , and the eigenvalue μ . Further discussion of this eigenvalue problem is given in Sec. III C and also in Sec. IV.

Thus, for each m , σ , and μ , there will be a corresponding regular solution $\mathbf{D}_\mu^{m\sigma}$ of the axisymmetric wave equation. Thus

$$\mathbf{D}_\mu^{m-} = \sum_{l \text{ odd}} d_{lm}^-(\mu) \mathbf{C}_{lm}(q\mathbf{r}) + \sum_{l \text{ even}} d_{lm}^-(\mu) \mathbf{A}_{lm}(q\mathbf{r}) \quad (3.13)$$

and

$$\mathbf{D}_\mu^{m+} = \sum_{l \text{ odd}} d_{lm}^+(\mu) \mathbf{A}_{lm}(q\mathbf{r}) + \sum_{l \text{ even}} d_{lm}^+(\mu) \mathbf{C}_{lm}(q\mathbf{r}). \quad (3.14)$$

The corresponding electric field is found from (3.5). Using (3.7), we can write

$$\mathbf{E}_\mu^{m\sigma} = \frac{1 + \tilde{\gamma}\mu}{\tilde{\epsilon}} \mathbf{D}_\mu^{m\sigma} + \frac{\tilde{\gamma}}{\tilde{\epsilon}} \sum_l [l(l+1)]^{-1/2} \Delta_{lm}^\sigma(\mu) \mathbf{B}_{lm}(q\mathbf{r}), \quad (3.15)$$

where

$$\Delta_{lm}^\sigma(\mu) = \begin{cases} \sqrt{l(l+1)} \sum_{l'} (S_{l'l}^m + Q_{l'l}^m) d_{l'm}^\sigma, & \sigma = (-1)^{l+1} \\ 0, & \sigma = (-1)^l. \end{cases} \quad (3.16)$$

The subscripts $\sigma = (-1)^{l+1}$ and $(-1)^l$ on the left-hand side of Eq. (3.16) mean that, if σ is even, then for even l the quantity $\Delta_{lm}^\sigma(\mu)$ is given by upper expression (3.16) and for odd l it is given by the lower one; for odd σ the meaning is just the reverse.

The corresponding magnetic field is obtained from the first of Eqs. (2.1), using the formulas (2.16) for the curl of vector spherical waves,

$$\mathbf{B}_\mu^{m-} = \left[\frac{\omega}{qc} \right] \left[- \sum_{l \text{ odd}} d_{lm}^-(\mu) \mathbf{A}_{lm}(q\mathbf{r}) + \sum_{l \text{ even}} d_{lm}^-(\mu) \mathbf{C}_{lm}(q\mathbf{r}) \right] \quad (3.17)$$

and

$$\mathbf{B}_\mu^{m+} = \left[\frac{\omega}{qc} \right] \left[\sum_{l \text{ odd}} d_{lm}^+(\mu) \mathbf{C}_{lm}(q\mathbf{r}) - \sum_{l \text{ even}} d_{lm}^+(\mu) \mathbf{A}_{lm}(q\mathbf{r}) \right]. \quad (3.18)$$

The symbol used here, $\mathbf{B}_\mu^{m\sigma}$, for the magnetic field should not be confused with the symbol \mathbf{B}_{lm} for the spherical waves.

This completes the construction of solutions of the axisymmetric wave equation (2.8) in spherical coordinates. The general solution within the cavity will be a superposition of the solutions that we have found.

B. Satisfying the boundary conditions

We shall now construct solutions in the interior of the sphere that will satisfy the boundary conditions (2.9). The electric displacement vector \mathbf{D} inside the sphere must be a linear combination of solutions (3.13) and (3.14), for fixed m and σ , of the vector-wave equation (2.4). Since the boundary-value problem is invariant under rotations about the z axis and spatial inversions, the solutions within the sphere will be characterized by the parameters m and σ . Therefore, for the solution inside the sphere, we will have the form

$$\mathbf{D}^{m\sigma}(\mathbf{r}) = \sum_\mu \left[\frac{cq}{\omega} \right] G^{m\sigma}(\mu) \mathbf{D}_\mu^{m\sigma}(\mathbf{r}). \quad (3.19)$$

The coefficients $G^{m\sigma}(\mu)$ are determined by the boundary conditions at the surface of the sphere. The corresponding superpositions for the electric and magnetic fields are

$$\mathbf{E}^{m\sigma}(\mathbf{r}) = \sum_\mu \left[\frac{cq}{\omega} \right] G^{m\sigma}(\mu) \mathbf{E}_\mu^{m\sigma}(\mathbf{r}) \quad (3.20)$$

and

$$\mathbf{B}^{m\sigma}(\mathbf{r}) = \sum_\mu \left[\frac{cq}{\omega} \right] G^{m\sigma}(\mu) \mathbf{B}_\mu^{m\sigma}(\mathbf{r}), \quad (3.21)$$

where $\mathbf{E}_\mu^{m\sigma}$ and $\mathbf{B}_\mu^{m\sigma}$ are given by Eqs. (3.16), (3.18), and (3.19). We have chosen the factor cq/ω for convenience.

Using the formulas (3.9) and the orthogonality of the vector spherical harmonics, the continuity of the tangential component of the electric field at the surface gives

$$\sum_\mu \chi_l^{m\sigma}(\mu) G^{m\sigma}(\mu) = 0, \quad l = 1, 2, \dots, \quad (3.22)$$

where

$$\chi_l^{m\sigma}(\mu) = \begin{cases} (1 + \tilde{\gamma}\mu) d_{lm}^\sigma(\mu) \alpha_l(x) - \tilde{\gamma} \Delta_{lm}^\sigma(\mu) \beta_l(x), & \sigma = (-1)^{l+1} \\ (1 + \tilde{\gamma}\mu) d_{lm}^\sigma(\mu) x \beta_l(x), & \sigma = (-1)^l, \end{cases} \quad (3.23a)$$

$$(3.23b)$$

and we have introduced

$$x = qa, \quad (3.24)$$

where q is given by (3.8), to simplify the notation. For each m and σ these equations are an infinite set of homogeneous linear equations for the coefficients $G^{m\sigma}(\mu)$. For a nontrivial solution to Eqs. (3.22) to exist, the determinant of the coefficients must be zero. The quantities

$\chi_l^{m\sigma}(\mu)$ may be considered as the elements of a matrix $\chi^{m\sigma}$ whose rows are labeled by l and whose columns are labeled by μ . The condition for the existence of solutions to Eqs. (3.22) may then be expressed formally as

$$\det(\chi^{m\sigma})=0. \quad (3.25)$$

This condition gives the resonant frequencies of the sphere.

The continuity of the normal component of the magnetic field requires $\hat{\mathbf{r}} \cdot \mathbf{B}|_{r=a}=0$. However, this condition does not lead to an independent equation, since the normal modes automatically satisfy this boundary condition.

Before leaving this section, we should like to emphasize that the solution presented so far is a formal one. Since μ is a continuous parameter, the sums over μ are, in fact, integrals. This poses the problem of how to interpret the quantities $\chi^{m\sigma}(\mu)$ or the determinant appearing in Eq. (3.25). We shall address these issues in the next section, where we discuss the numerical solution of the problem.

C. Auxiliary eigenvalue problem

The auxiliary eigenvalue problem (3.11) can be solved exactly. The eigenvalues μ are continuously distributed in the interval $0 \leq \mu \leq 1$. There are two distinct classes of eigenvectors: those associated with $\mu=0$ and those associated with $\mu \neq 0$. For $\mu=0$ the eigenvectors are

$$d_{lm}^\sigma(\theta) = (i)^l (-1)^m \left[\frac{(2l+1)(l-m)!}{4\pi l(l+1)(l+m)!} \right]^{1/2} \times \begin{cases} \sin^2 \theta \frac{dP_l^m}{d(\cos \theta)}, & \sigma = (-1)^l \\ imP_l^m, & \sigma = (-1)^{l+1}, \end{cases} \quad (3.26a)$$

$$(3.26b)$$

where $\pi/2 \leq \theta \leq \pi$. For $\mu \neq 0$ the eigenvectors are

$$d_{lm}^\sigma(\theta) = (i)^l (-1)^m \left[\frac{(2l+1)(l-m)!}{4\pi l(l+1)(l+m)!} \right]^{1/2} \times \begin{cases} imP_l^m, & \sigma = (-1)^l \\ -\sin^2 \theta \frac{dP_l^m}{d(\cos \theta)}, & \sigma = (-1)^{l+1}, \end{cases} \quad (3.27a)$$

$$(3.27b)$$

where $0 \leq \theta \leq \pi/2$. Here $P_l^m \equiv P_l^m(\cos \theta)$ is the associated Legendre function and the eigenvalue μ is given by

$$\mu = \begin{cases} 0 & \text{for } \frac{\pi}{2} \leq \theta \leq \pi, \\ \sin^2 \theta & \text{for } 0 \leq \theta \leq \frac{\pi}{2}. \end{cases} \quad (3.28a)$$

$$(3.28b)$$

We note that there is an infinite degeneracy for $\pi/2 \leq \theta \leq \pi$ since, for this range of θ , μ is identically zero. However, this degeneracy is not carried over to the electric and magnetic fields since the corresponding eigenvectors

$d_{lm}^\sigma(\mu=0)$ are all different. The $\mu=0$ eigenvalue has the additional property that the quantity $\Delta_{lm}^\sigma(\mu=0)$ is identically zero; i.e., for the $\mu=0$ eigenvalue, the electric field [Eq. (3.15)] has no longitudinal component.

These eigenvectors are closely related to the functions $d_{m',m}^{(j)}$ that occur in the irreducible representations of finite rotations.⁸ The fact that Eqs. (3.26) and (3.27) solve the eigenvalue problem (3.11) may be verified by direct substitution into Eq. (3.11) and using the recurrence relations for the Legendre polynomials. We obtained this solution by expanding the fields inside the sphere in terms of the plane-wave solutions of the axisymmetric wave equation (2.8), expanding the plane waves in terms of vector spherical waves, fitting the boundary conditions, and finally comparing with the equations obtained in Sec. III B.¹²

The spectrum of eigenvalues being continuous, the sum over μ appearing in Sec. III B should be interpreted as an integral, a convenient choice being

$$\sum_{\mu} \rightarrow \int_0^{\pi} d\theta. \quad (3.29)$$

For a given m and σ the eigenvectors given in (3.26) and (3.27) form a complete orthonormal set of functions in the interval $[0, \pi]$ and thus

$$\sum_l d_{lm}^\sigma(\theta) d_{lm}^\sigma(\theta') = \delta(\theta - \theta'), \quad (3.30)$$

$$\int_0^{\pi} d\theta d_{lm}^\sigma(\theta) d_{l'm}^\sigma(\theta) = \delta_{ll'},$$

where $\delta(\theta - \theta')$ is the Dirac δ . (The orthogonality for different m and σ is a consequence of the orthogonality properties of the vector spherical waves.)

IV. NUMERICAL RESULTS

In this section we shall discuss our method for the numerical evaluation of the normal-mode frequencies and the associated electric-field lines. In Sec. IV A we give the basic equations and outline the algorithm for the computation of the normal-mode frequencies. This algorithm will be based on successive truncations of the infinite-dimensional equations of Sec. III. In Sec. IV B we present the results of our numerical calculations for the normal-mode frequencies. Plots of these frequencies as a function of dielectric asymmetry will be given and discussed. In Sec. IV C we calculate the electric-field lines for the lowest modes of the cavity and compare them with the lowest modes of the Macdonald problem. Graphs of the field lines for several values of $\bar{\gamma}$ are presented and discussed.

A. Algorithm

In the evaluation of the infinite determinant (3.25), we are faced with the problem of columns that are labeled by the continuous index μ . To resolve this difficulty we have used a method that turns out to be computationally simple and efficient. The basis of our algorithm is replacing the expansion (3.1) for the electric displacement field \mathbf{D} by a finite sum. Thus all the infinite sums over l and l'

are to be replaced by finite sums from $l = l_{\min}$ to $l = l_{\max}$, where l_{\min} is the larger of m and 1. Thus the infinite determinant in Eq. (3.25) (Ref. 13) may be evaluated by successive truncations. The parameter l_{\max} characterizes the truncations; successive truncations correspond to increasing l_{\max} . We truncate the eigenvalue problem (3.11) by replacing the matrices by their $N \times N$ upper-left corner, where $N = l_{\max} - l_{\min} + 1$. The parameter N determines the order of approximation. As N is increased, the accuracy of the calculation increases. Then the infinite-dimensional eigenvalue problem (3.11) becomes

$$\sum_{l'=l_{\min}}^{l_{\max}} (\mathcal{N}_{ll'}^{m\sigma} - \mu \delta_{ll'}) d_{l'm}^{\sigma} = 0, \quad l = l_{\min}, l_{\min} + 1, \dots, l_{\max}. \quad (4.1)$$

Since the matrix $\mathcal{N}^{m\sigma}$ is a real symmetric $N \times N$ matrix, it follows that there will be N distinct eigenvectors $d_{lk}^{m\sigma}$ ($k = 1, 2, \dots, N$), where we have used the notation $d_{lm}^{\sigma}(\mu_k) \equiv d_{lk}^{m\sigma}$. The corresponding eigenvalues μ_k will be real and discrete and will fall in the region $0 \leq \mu \leq 1$, i.e., within the spectrum of the exact solution. For each truncation of size N , it turns out that there is one $[(N-1)/2]$ -fold degenerate zero eigenvalue and $[(N+1)/2]$ distinct positive eigenvalues. We note here that the number of distinct eigenvectors with eigenvalue $\mu = 0$ is equal to the multiplicity of the eigenvalue 0.

In the truncated problem, the eigenvectors satisfy the orthogonality and completeness relations

$$\begin{aligned} \sum_{l=1}^N d_{lm}^{\sigma}(\mu_k) d_{lm}^{\sigma}(\mu_{k'}) &= \delta_{kk'}, \\ \sum_{k=1}^N d_{lm}^{\sigma}(\mu_k) d_{l'm}^{\sigma}(\mu_k) &= \delta_{ll'}. \end{aligned} \quad (4.2)$$

As N becomes large, the eigenvalues fill the interval $0 \leq \mu_k \leq 1$ densely, and the corresponding eigenvectors become asymptotically equivalent to Eqs. (3.26) and (3.27), aside from normalization factors.

Next, we approximate the infinite set of Eqs. (3.22) by the finite set of equations

$$\sum_{k=1}^N \chi_{lk}^{m\sigma} G_k^{m\sigma} = 0, \quad l = l_{\min}, \dots, l_{\max} \quad (4.3)$$

where

$$\chi_{lk}^{m\sigma} \equiv \chi_l^{m\sigma}(\mu_k), \quad G_k^{m\sigma} \equiv G^{m\sigma}(\mu_k). \quad (4.4)$$

Note that $\chi^{m\sigma}$ is now a real, but not symmetric, square $N \times N$ matrix. The resonant frequencies are then given by the condition

$$\det(\chi^{m\sigma}) = 0, \quad (4.5)$$

which is an $N \times N$ determinant.

In the numerical solution of the (finite) auxiliary eigenvalue (4.1), we have taken advantage of standard subroutines.¹⁴

We have tested the convergence of our method by comparing the successive values of the same root as the

truncation size was increased. In practice, reasonable numerical convergence is usually achieved for N as low as 3. However, to get accurate results, especially near the limit $\bar{\gamma} = -1$, we have used N as large as 17. There is a limit beyond which further increase in the truncation size worsens the convergence since rounding errors become important. We reached this limit for the truncation size $N \approx 21$. Our accuracy, based on how much a typical root changed in successive truncations, was about 1 part in 10^6 .

This algorithm was implemented both on a Digital Equipment Corporation VAX-8600 using FORTRAN. The calculation of a single normal-mode frequency (in double precision), for $N = 9$, took 2 s of CPU time. Convergence occurs more rapidly for the lower modes of the cavity than the higher ones. When two modes become very close to each other, the interference between them increases the computational effort considerably. Moreover, as $\bar{\gamma} \rightarrow -1$, the determinant of the matrix of the coefficients becomes very small and rescaling the determinant becomes necessary.

B. Normal-mode frequencies

We have computed the normal-mode frequencies in the form of the quantities

$$x = \sqrt{\epsilon_{xx}} \left[\frac{\omega a}{c} \right], \quad (4.6)$$

for $m = 0, 1, 2, 3$ and $l_{\max} = 7$. Note that x is, in fact, the output of our numerical solution. We may designate the modes by the $x_{m\sigma n}$. Here m is the azimuthal number, taking the values $0, \pm 1, \pm 2, \dots$, $\sigma = \pm$ is the parity, and n indicates the n th root of the determinant in Eq. (4.5).

The results of these numerical calculations are displayed in Figs. 1–6. All throughout our numerical calculations, we have set $a = 1$ and $\bar{\epsilon} = 1$. Thus the resonant frequencies are given in units of $c/a\sqrt{\bar{\epsilon}}$. We have displayed the normal-mode wave numbers in the range $0 \leq x \leq 8$ for the interval $-1 \leq \bar{\gamma} \leq 1$.

In Fig. 1 we have plotted the normal-mode wave num-

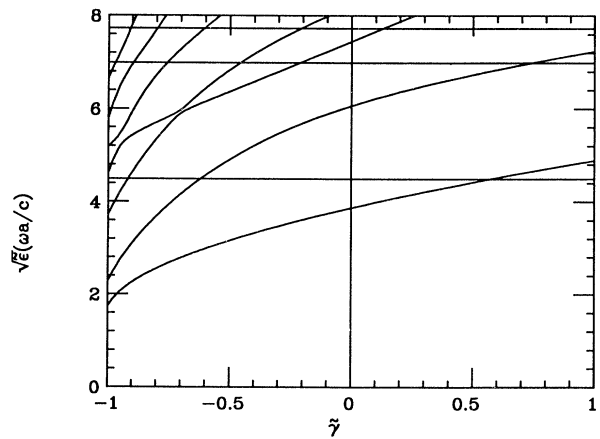


FIG. 1. Normal-mode frequencies $x_{m\sigma n}$ for an axisymmetric spherical-cavity resonator as a function of $\bar{\gamma}$, with $m = 0$ and $\sigma = \text{odd}$.

bers for $m = 0$ and $\sigma = \text{odd}$. We first note the existence of normal-mode frequencies that do not vary with $\tilde{\gamma}$. In fact, the existence of modes that are independent of $\tilde{\gamma}$ is a common feature of $m = 0$, $\sigma = \pm$, corresponding to an electric field that has no z component. We shall designate these modes by a prime and write $x'_{0\sigma n}$, where n refers to the n th constant resonant frequency.

Next, we note the existence of modes that vary as $\tilde{\gamma}$ is varied. These modes are monotonically increasing functions of $\tilde{\gamma}$. As $\tilde{\gamma}$ is increased, they increase without bound. Finally, we observe that as we reach the limit $\tilde{\gamma} = -1$ all the normal-mode frequencies go to finite limits.

Moving on to Fig. 2, where we have displayed the resonant frequencies for $m = 0$ and $\sigma = \text{even}$, we note the similarities between Figs. 2 and 1, that there are modes which are strongly dependent on $\tilde{\gamma}$ and that again there exist modes that are independent of $\tilde{\gamma}$. A feature of the $\tilde{\gamma}$ -dependent normal-mode frequencies is that, although they come very close to one another, they never cross; they repel one another. The close encounter of the modes and their mutual repulsion is a common feature in all of our graphs.

There is a striking difference between Figs. 1 and 2 in the behavior of the resonant frequencies at the limit that $\tilde{\gamma} = -1$. In contrast to the odd-parity case, the even-parity modes approach zero (with the exception of the constant modes) as $\tilde{\gamma} \rightarrow 0$. To exhibit this phenomenon more clearly, we have enlarged the region around $\tilde{\gamma} = -1$ and have plotted the six lowest nonconstant modes in Fig. 3. We have plotted the modes against $(1 + \tilde{\gamma})^{1/2}$ to remove the curvature in these lines. It can clearly be observed that the resulting straight lines do indeed go through zero as $\tilde{\gamma} \rightarrow -1$. We conclude that at this limit all nonconstant roots approach zero. We remark here that this phenomena causes the upper-left corner of Fig. 2 to be densely covered with lines going to zero. In order to avoid cluttering the figures, we have chosen not to display all these lines. This same phenomena is present

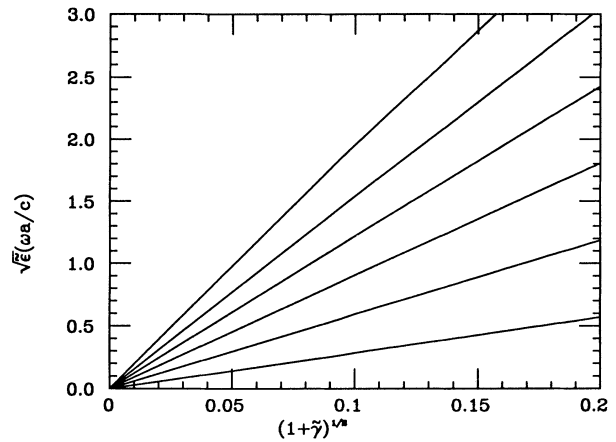


FIG. 3. Lowest normal-mode frequencies x_{0+n} for an axisymmetric spherical-cavity resonator as a function of $(1 + \tilde{\gamma})^{1/2}$.

for other values of m and the parameter σ , as we shall see.

In Fig. 4 we have displayed the results of our numerical computations for the case $m = 1$ and $\sigma = \text{odd}$. All modes are strongly dependent on $\tilde{\gamma}$, the reason being that the corresponding electric field has a component along the z axis. Every time that two or more modes approach each other, they also subsequently repel each other. This is similar to what we saw earlier in Figs. 1 and 2. In addition, as the limit $\tilde{\gamma} = -1$ is reached, all normal-mode frequencies become zero.

We have plotted the normal-mode wave numbers for $m = 1$, $\sigma = \text{even}$ in Fig. 5. We observe the same features as seen previously. The general features of the modes for higher values of m are quite similar to the cases discussed so far. Our numerical results seem to indicate that the normal-mode frequencies go to zero at the $\tilde{\gamma} = -1$ limit according to the simple rule $\sigma = (-1)^m$.

The constant modes appear only for $m = 0$, $\sigma = \pm$,

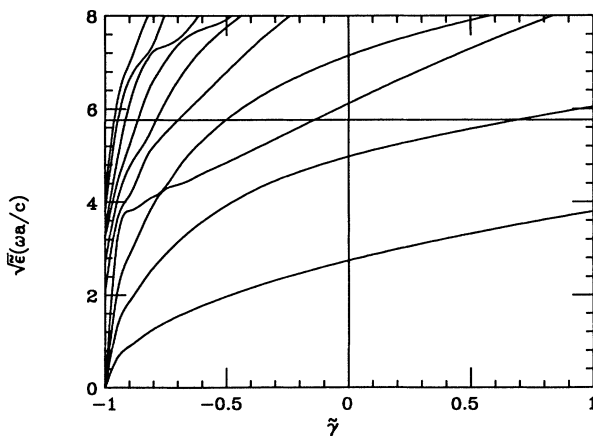


FIG. 2. Normal-mode frequencies $x_{m\sigma n}$ for an axisymmetric spherical-cavity resonator as a function of $\tilde{\gamma}$, with $m = 0$ and $\sigma = \text{even}$.

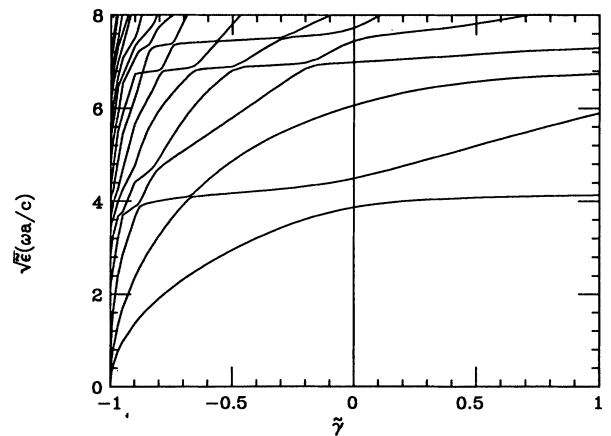


FIG. 4. Normal-mode frequencies $x_{m\sigma n}$ for an axisymmetric spherical-cavity resonator as a function of $\tilde{\gamma}$, with $m = 1$ and $\sigma = \text{odd}$.

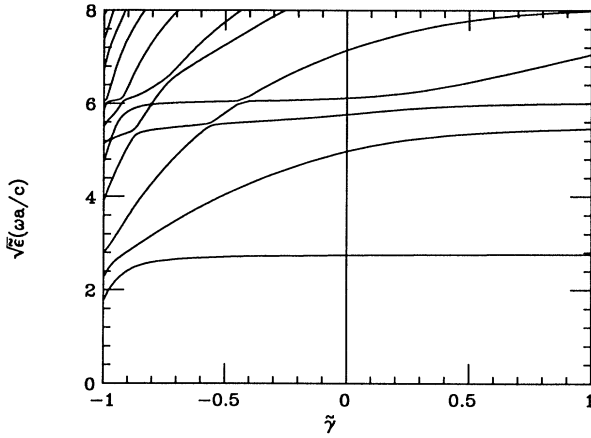


FIG. 5. Normal-mode frequencies $x_{m\sigma n}$ for an axisymmetric spherical-cavity resonator as a function of $\tilde{\gamma}$, with $m = 1$ and $\sigma = \text{even}$.

which may be understood by writing out the determinant of the matrix $\chi^{m\sigma}$ for $m = 0$ case explicitly and by noting that the resulting determinant factorizes into a product of spherical Bessel functions $j_l(x)$ multiplied by a determinant of lower rank. The product of the spherical Bessel functions will be independent of $\tilde{\gamma}$, while the determinant will be a function of $\tilde{\gamma}$.

These graphs of normal-mode frequencies versus $\tilde{\gamma}$ indicate that the classification of modes into TE and TM is no longer possible since, for a given parity σ , the TE and TM modes are mixed. Therefore, we classify the modes according to parameters m , σ , and n , where n indicates the n th root of $\det(\chi^{m\sigma})$. The lowest-lying mode for $m = 0$ and $\sigma = +$ is still the lowest mode for all values of m and σ . This is the fundamental mode of the cavity, a situation similar to the Macdonald's case. The azimuthal symmetry of the problem implies that the normal modes are doubly degenerate, corresponding to $+m$ and $-m$ modes.

C. Electric-field lines

The electric-field lines (electric lines of force) are defined to be everywhere tangent to the \mathbf{E} field vector and to have the same direction. The equation for the (electric-) field lines is then

$$\frac{d\hat{\mathbf{r}}}{ds} = \frac{\mathbf{E}}{E}. \quad (4.7)$$

Here s is the arc length along the field line and E is the magnitude of the electric-field vector. Similar definitions hold for the electric displacement field \mathbf{D} and the magnetic field \mathbf{B} .

Our method of numerical solution of Eq. (4.7) for the electric-field lines is similar to the successive truncation method discussed in Sec. IV A. We replace the infinite expansion (3.19) for the odd- and even-parity electric displacement vector \mathbf{D} with finite sums up to N . In the calculation of these sums, we need the expansion coefficients $G^{m\sigma}(\mu)$. These are the solutions to the truncated equa-

tion (4.3). We evaluate the $G^{m\sigma}(\mu)$ by imposing the constraint

$$\sum_{k=1}^N G_k^{m\sigma} = 1. \quad (4.8)$$

This corresponds to fixing the normalization of the expansion coefficients. Next, we use the dielectric relation (2.6) to compute the corresponding electric field. Then, having the electric field at hand, we calculate the field lines.

We have used a fourth-order Runge-Kutta method¹⁴ to integrate Eq. (4.6). These computations were performed on the VAX-8600 in double precision. It takes about 7 s of CPU time on the VAX to calculate a single field line for a typical value of $\tilde{\gamma}$ and $N = 9$.

It is difficult to give a general rule for the speed of convergence in this problem. However, a number of reasonably general statements can be made. As the parameter $\tilde{\gamma}$ increases (decreases), progressively larger truncations must be used. Moreover, the computation of higher multipole field lines requires larger truncations. We have observed that convergence occurs more rapidly for the fundamental mode than for any other mode. But for all the modes, convergence for the field lines occurs at larger truncations than for the corresponding normal mode.

We have computed the electric-field lines for $m = 0$ and $\sigma = +$ and $-$. We have only considered those modes for which the frequency is a function of $\tilde{\gamma}$. For the constant $\tilde{\gamma}$ modes of axisymmetric cavity, the field lines (both electric and magnetic) are given by the corresponding TE field lines of Macdonald with $m = 0$ and an effective dielectric constant $\tilde{\epsilon}$.

For $\tilde{\gamma}$ -dependent modes, the magnetic field will be purely planar; the magnetic-field lines will be circles centered around the z axis. The electric field, on the other hand, will have a z component and the electric-field lines will vary as $\tilde{\gamma}$ is varied. We have plotted the field lines for three values of $\tilde{\gamma}$: $\tilde{\gamma} = 0$ (the Macdonald field lines), $\tilde{\gamma} = -0.9$, and $\tilde{\gamma} = 1$, in Figs. 6(a), 6(b), and 6(c). We have plotted the field lines for the isotropic (Macdonald) case so as to be able to show more clearly the effect of varying $\tilde{\gamma}$. These plots are the projections of the field lines onto the xz plane.

There are two limits that are of interest: $\tilde{\gamma} \rightarrow -1$ and $\tilde{\gamma} \rightarrow \infty$. In the first limit the material is conducting along the z axis and insulating in the xy plane. Note that at this limit the electric displacement field has no z component; it lies completely in the xy plane. The other limit, on the other hand, is the opposite limit in which the material inside the sphere is insulating along the z axis and conducting in the xy plane.

In Fig. 6(a) we have plotted the field lines for the fundamental mode of the cavity at $\tilde{\gamma} = 0.9, 0$, and 1 . The middle figure shows the field lines of the isotropic cavity $\tilde{\gamma} = 0$. This is the TM_{11} mode with $q_0 a = 2.74$. The field lines are exactly the same as those that one obtains, for the fundamental mode, in the Macdonald problem.¹¹ The field lines are perpendicular at the surface since the tangential component of the electric field must vanish there. The top part of Fig. 6(a) shows the change in the

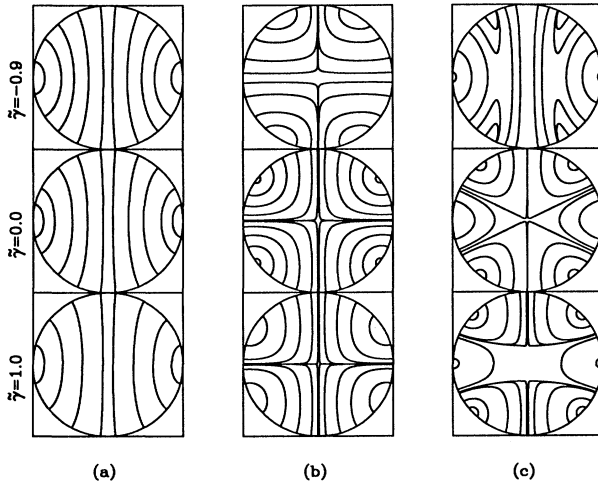


FIG. 6. Electric-field lines for $m=0$ modes of the cavity: (a) field lines for the fundamental mode of the cavity with $\sigma=\text{even}$, (b) field lines for the next higher mode of the cavity with $\sigma=\text{odd}$, and (c) field lines for the second higher mode of the cavity with $\sigma=\text{even}$.

fundamental mode when we approach the $\tilde{\gamma}=-1$ limit. The field lines are plotted for $\tilde{\gamma}=-0.9$, with $q_0a=0.897$. The field lines have become more curved so as to counter the large conductivity along the z axis. We infer that at $\tilde{\gamma}=-1$ the field lines will be parallel to the xy plane since at this limit the electric field has no z component. In the bottom part of Fig. 6(a), we observe the effect of having a large $\tilde{\gamma}$. We have plotted the field lines of the fundamental mode for $\tilde{\gamma}=1$ and $q_0a=3.797$. As $\tilde{\gamma}$ becomes larger and larger, the material will behave more and more like a stack of parallel-plate capacitors. The field lines will become more and more straight as we approach the limit $\tilde{\gamma}\rightarrow\infty$.

In the middle part of Fig. 6(b), we have displayed the first odd-parity mode for $\tilde{\gamma}=0$ and $q_0a=3.87$, i.e., the second mode of the isotropic cavity, TM_{21} . We note that there are four nodes present in Fig. 6(b). As $\tilde{\gamma}$ is varied, these regions remain distinct. The top part of Fig. 6(b) shows the field lines for the first higher odd-parity mode with $\tilde{\gamma}=-0.9$ and $q_0a=2.254$. The bottom part of Fig. 6(b), on the other hand, shows the effect on the field lines when $\tilde{\gamma}$ is increased. Here we have plotted the field lines for the first odd-parity mode with $\tilde{\gamma}=1$ and $q_0a=4.891$. As we approach infinity, we should expect to see more parallel field lines along the z axis. At both limits, $\tilde{\gamma}=-1$ and ∞ , we expect to see the curved lines to have 90° elbows, indicating the marked difference in material properties in different directions.

The field lines for the first even-parity mode are plotted in Fig. 6(c). In the middle part of Fig. 6(c), we have plotted the TM_{31} mode of the isotropic cavity with $q_0a=4.97$. The top part of the figure shows the field lines with $\tilde{\gamma}=-0.9$ and $q_0a=1.86$. At $\tilde{\gamma}=-1$, we should then expect the bulk of field lines to be straight lines going from top to bottom with a few curved ones crowded to the sides. In the bottom part of the figure, we

have plotted the field lines with $\tilde{\gamma}=1$ and $q_0a=6.044$. In the limit that $\tilde{\gamma}=\infty$, we should expect to see very sharp turns in the elbows of the field lines. Moreover, we expect to see six sharply defined regions that are separated by curves that have acute angle elbows.

V. SUMMARY AND CONCLUSIONS

In this paper we have formally solved the problem of the resonant frequencies of a metallic sphere filled with an axisymmetric material and evaluated those frequencies numerically. The complexity of the problem arises from the fact that the axisymmetric wave equation [Eq. (2.8)] is not separable in spherical coordinates.

Our technique for solution has involved the following steps.

(i) Inside the sphere we chose to solve for the electric displacement vector \mathbf{D} . We expanded \mathbf{D} in terms of vector spherical waves \mathbf{A}_{lm} and \mathbf{C}_{lm} [Eq. (3.1)].

(ii) We found in order for this expansion to be a solution of the axisymmetric wave function, special conditions on the expansion coefficients a_{lm} and c_{lm} must be satisfied. We found that these special conditions could be cast in the form of an auxiliary eigenvalue problem [Eq. (3.11)] in which the components of the eigenvectors d_{lm}^σ were a_{lm} and c_{lm} and the eigenvalues μ determined the spectrum of the allowed wave numbers q [Eq. (3.8)] inside the sphere. The solutions to this eigenvalue problem were found to be separable into results of even and odd parity ($\sigma=\pm 1$).

(iii) Thus, for each eigenvalue μ , magnetic quantum number m , and parity σ , we found a solution $\mathbf{D}_{\mu}^{m\sigma}$ of the axisymmetric wave equation [Eqs. (3.13) and (3.14)]. The general solution, therefore, involves a sum over all these solutions, in which we called the expansion coefficients $G^{m\sigma}(\mu)$.

(iv) The electric field \mathbf{E} and magnetic field \mathbf{B} could then be written down using the inverse dielectric relation $\mathbf{E}=(\tilde{\epsilon}^{-1}\cdot\mathbf{D})$ and Faraday's law [Eq. (2.1)], respectively.

(v) The boundary conditions were applied in Sec. III B. There we required (a) continuity of the normal component of \mathbf{D} and (b) continuity of the tangential component of \mathbf{E} . The application of these boundary conditions led to four scalar equations for the unknown coefficients $G^{m\sigma}(\mu)$ inside the sphere. Only two of these equations were independent.

(vi) These equations were, in fact, found to be matrix equations of infinite size. We outlined a numerical technique for their solution in Sec. IV A, using the method of successive truncations. The roots of the determinant of the coefficients were the resonant frequencies of the sphere. We also gave results of our numerical computation of these modes and the corresponding field lines.

There are a number of directions where extensions of this work may prove interesting and useful: (i) calculation of the normal modes for an ellipsoidal resonator, (ii) investigation of the changes in the normal modes when full dielectric anisotropy is included, and (iii) exploration of the possibility of mode conversion in axisymmetric resonators and its application to switching devices.

- ¹G. W. Ford and S. A. Werner, Phys. Rev. B **18**, 6752 (1978), and references cited therein.
- ²H. M. Macdonald, *Electric Waves* (Cambridge University Press, Cambridge, England, 1902), Chap. 16.
- ³D. M. Strayer, G. J. Dick, and E. Tward, IEEE Trans. Magn. **19**, 512 (1983).
- ⁴J. D. Jackson, *Classical Electrodynamics*, 2nd ed. (Wiley, New York, 1975), pp. 335 and 336.
- ⁵*Handbook of Mathematical Functions*, edited by M. Abramowitz and I. A. Stegun (Dover, New York, 1965), Chap. 9.
- ⁶P. M. Morse and H. F. Feshbach, *Methods of Theoretical Physics* (McGraw-Hill, New York, 1953), Vol. II, Sec. 13.3.
- ⁷Reference 5, Chap. 10.1
- ⁸A. R. Edmonds, *Angular Momentum in Quantum Mechanics* (Princeton University Press, Princeton, NJ, 1951).
- ⁹G. W. Ford and S. A. Werner, Phys. Rev. B **8**, 3717 (1973). Also see Ref. 6, pp. 81–85; J. M. Blatt and V. F. Weiskopf, *Theoretical Nuclear Physics* (Wiley, New York, 1952), Appendix B.
- ¹⁰Reference 1, Eqs. (3.8).
- ¹¹J. A. Stratton, *Electromagnetic Theory* (McGraw-Hill, New York, 1941), pp. 560–563.
- ¹²In Ref. 1, if we allow $\tilde{W}\lambda \rightarrow 0$ for $\pi/2 \leq \theta \leq \pi$ and $\tilde{W}\lambda \rightarrow i\tilde{\gamma} \sin^2\theta$ for $0 \leq \theta \leq \pi/2$, we recover the same eigenvectors.
- ¹³R. Courant and D. Hilbert, *Methods of Mathematical Physics*, 1st English ed. (Interscience, New York, 1953), Vol. I, Chap. III.
- ¹⁴W. H. Press, et al., *Numerical Recipes* (Cambridge University Press, Cambridge, England, 1986).